AEM
Journals.ASM.org

High-Resolution Analysis of Gut Environment and Bacterial Microbiota Reveals Functional Compartmentation of the Gut in Wood-Feeding Higher Termites (*Nasutitermes* spp.)

Tim Köhler,[a] Carsten Dietrich,[a] Rudolf H. Scheffrahn,[b] and Andreas Brune[a]

Max Planck Institute for Terrestrial Microbiology, Marburg, Germany,[a] and Fort Lauderdale Research and Education Center, University of Florida, Davie, Florida, USA[b]

Higher termites are characterized by a purely prokaryotic gut microbiota and an increased compartmentation of their intestinal tract. In soil-feeding species, each gut compartment has different physicochemical conditions and is colonized by a specific microbial community. Although considerable information has accumulated also for wood-feeding species of the genus *Nasutitermes*, including cellulase activities and metagenomic data, a comprehensive study linking physicochemical gut conditions with the structure of the microbial communities in the different gut compartments is lacking. In this study, we measured high-resolution profiles of H_2, O_2, pH, and redox potential in the gut of *Nasutitermes corniger* termites, determined the fermentation products accumulating in the individual gut compartments, and analyzed the bacterial communities in detail by pyrotag sequencing of the V3-V4 region of the 16S rRNA genes. The dilated hindgut paunch (P3 compartment) was the only anoxic gut region, showed the highest density of bacteria, and accumulated H_2 to high partial pressures (up to 12 kPa). Molecular hydrogen is apparently produced by a dense community of *Spirochaetes* and *Fibrobacteres*, which also dominate the gut of other *Nasutitermes* species. All other compartments, such as the alkaline P1 compartment (average pH, 10.0), showed high redox potentials and comprised small but distinct populations characteristic for each gut region. In the crop and the posterior hindgut compartments, the community was even more diverse than in the paunch. Similarities in the communities of the posterior hindgut and crop suggested that proctodeal trophallaxis or coprophagy also occurs in higher termites. The large sampling depths of pyrotag sequencing in combination with the determination of important physicochemical parameters allow cautious conclusions concerning the functions of particular bacterial lineages in the respective gut sections to be drawn.

Termites contribute substantially to the turnover of carbon and nitrogen in tropical ecosystems (30). Their diet consists exclusively of lignocellulose in various stages of decomposition, ranging from sound wood to humus (4). The digestion of this recalcitrant diet relies on the metabolic activities of a dense and diverse intestinal microbiota (13). In the evolutionarily lower termites, flagellate protists hydrolyze the wood and ferment the resulting monomers, but in higher termites, these cellulolytic symbionts are lacking (see reference 13 and references therein). Although the endoglucanases in the midgut region are secreted by the host epithelium, the cellulolytic activities in the hindgut of higher termites seem to be of bacterial origin (70, 74).

In many higher termites, the hindgut is strongly compartmentalized (44), forming several consecutive microbial bioreactors, some of which are extremely alkaline (5, 12). The hindgut microbiota of wood-feeding *Microcerotermes* and *Nasutitermes* spp. is dominated by *Spirochaetes*, *Fibrobacteres*, and members of the candidate phylum TG3 (26, 27). A metagenomic analysis of the microbiota in the hindgut paunch (P3 compartment) of a *Nasutitermes* sp. implicated members of *Spirochaetes* and *Fibrobacteres* in the hydrolysis of wood (73). Although the presence of hydrogenase genes indicates the capacity of the gut microbiota to form or consume H_2, the presence of H_2 in the paunch or other sections of *Nasutitermes* spp., particularly the alkaline gut region (9), remains to be elucidated. The individual gut compartments of soil-feeding *Cubitermes* spp. (subfamily Termitinae) are colonized by different communities of bacteria and archaea (21, 61), and the alkaline P1 compartments of different higher termites harbor a similar bacterial microbiota (68). However, apart from a study of the bacteria colonizing the mixed segment of *Nasutitermes takasagoensis* (subfamily Nasutitermitinae) (71), information about the microbial communities in the different hindgut sections of wood-feeding higher termites and a highly resolved analysis of important physicochemical parameters in the different gut regions are lacking.

In this study, we combine microsensor measurements of physicochemical conditions (oxygen and hydrogen partial pressure, redox potential, and pH) with high-resolution profiles of the bacterial microbiota and their fermentation products in the different gut compartments of *Nasutitermes corniger*.

MATERIALS AND METHODS

Sample preparation. *Nasutitermes corniger* (Motschulsky) was taken from a laboratory nest (University of Florida) collected in Dania Beach, FL, from established field populations of this exotic arboreal termite, which is synonymous with *Nasutitermes costalis* (56, 57). *Nasutitermes takasagoensis* was collected on Iriomote Island, Japan, by Gaku Tokuda (University of the Ryukyus, Okinawa, Japan). Only worker caste termites were used for the experiments. After dissecting the termites with sterile, fine-tipped forceps, we used intact guts for microsensor studies of the individual compartments (Fig. 1). For metabolic profiles and pyrotag sequencing, we separated the guts, placed under a stereomicroscope, into six

Received 2 March 2012 Accepted 13 April 2012
Published ahead of print 27 April 2012
Address correspondence Andreas Brune, brune@mpi-marburg.mpg.de.
Supplemental material for this article may be found at http://aem.asm.org/.

doi:10.1128/AEM.00683-12

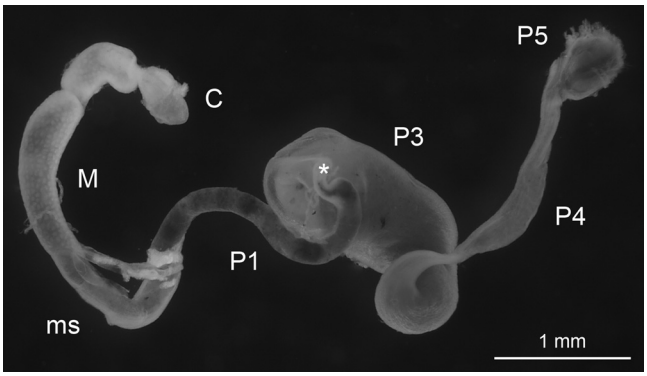

FIG 1 Intestinal tract of *Nasutitermes corniger*. The gut includes the crop (C), midgut (M), mixed segment (ms), and several hindgut segments (P1 to P5); the asterisk marks the position of the P2 (enteric valve).

major sections, comprising the crop, the midgut, and the four major hindgut compartments (P1, P3, P4, and P5), and homogenized them with sterile micropestles (Eppendorf, Hamburg, Germany). Because they are difficult to delineate, the mixed segment (ms) was included with the P1 compartment. To increase sensitivity of detection and to account for intraspecific variations, we always pooled an indicated number of gut sections (see below).

Microsensor measurements. All microsensors were purchased from Unisense (Aarhus, Denmark). Oxygen (OX-10) and hydrogen (H2-10) microsensors had tip diameters of ca. 10 μm and detection limits of ca. 0.02 and 0.04 kPa, respectively, and were polarized and calibrated as previously described (9, 18). The redox electrode (RD-10) had a tip diameter of ca. 10 μm, and the pH electrode (PH-10) had a tip diameter of 10 to 20 μm and a sensitive tip length of 100 to 150 μm; each was used together with an Ag-AgCl reference electrode and a high-impedance voltmeter. pH measurements were calibrated using standard curves obtained with commercial standard solutions of pH 4.0, 7.0, 9.0, and 11.0 (Carl Roth, Karlsruhe, Germany) as previously described (12). Redox measurements were calibrated using freshly prepared saturated quinhydrone solutions in pH standards at pH 4.0 and 7.0.

Microsensor profiles were measured in glass-faced microchambers as previously described (9). Freshly dissected guts of *N. corniger* were placed flat and fully extended onto a 4-mm layer of 2% (wt/vol) agarose and were covered with 0.5% (wt/vol) agarose (both made up with Ringer's solution). Microsensors were positioned using a manual micromanipulator (Märzhäuser, Wetzlar, Germany), and tip position was visually controlled with a horizontally mounted stereomicroscope (Zeiss, Jena, Germany); measurement commenced ca. 10 min after embedding and lasted less than 1 h.

Metabolite pools. Forty gut sections each of *N. corniger* were homogenized in 80 μl NaOH (10 mM), and metabolites in the clarified supernatants were analyzed using a combination of gas chromatography (GC) (66) and high-performance liquid chromatography (HPLC) (52), as previously described in detail.

Microbial cell counts. Twenty gut sections each of *N. corniger* were homogenized in 0.5 ml phosphate-buffered saline (PBS) (49) and fixed with 4% (vol/vol) formaldehyde at 4°C for 13 h. Microbial cells were counted using the procedure of Pernthaler et al. (50), but the sonication step was excluded. Samples were washed with PBS, and appropriate dilutions were filtered onto polycarbonate filters (pore size, 0.2 μm; GTTP; Millipore, Schwalbach/Ts., Germany) and stored at −20°C. For analysis, filters were stained with 4′,6′-diamidino-2-phenylindole (DAPI), washed with sterile water and then with 70% (vol/vol) ethanol, and embedded in Citifluor AF1 solution (Citifluor, London, United Kingdom). Microbial cells were counted at 1,000-fold magnification using a Zeiss Axiophot epifluorescence microscope equipped as previously described (61).

Primer design. Primers 341F (40) and 787R (29), targeting the V3-V4 region of the bacterial 16S rRNA gene, were modified on the basis of the sequence information in the SILVA 100 database (53), focusing on an optimal coverage of the taxa known to prevail in termite guts. Modifications were tested using the probe match function of ARB software (version 5.1) (39). The resulting primer set, 343Fmod (TACGGGWGGCW GCA) and 784Rmod (GGGTMTCTAATCCBKTT), showed perfect matches to 87% of the sequences in the database (90.5%, allowing one mismatch), and coverage was even higher in the phyla relevant to the termite gut environment (see Fig. S1 in the supplemental material).

Pyrotag sequencing. Twenty sections of each gut compartment of *N. corniger*, 10 hindguts (P1 to P5) of both *N. corniger* and *N. takasagoensis*, and 10 whole guts of *N. corniger* were each pooled and homogenized in PBS. DNA was extracted with phenol-chloroform using the bead-beating protocol described by Henckel et al. (25), precipitated with 2 volumes of polyethylene glycol, and amplified with the newly designed primers using a high-fidelity polymerase (Herculase II; Agilent, Waldbronn, Germany). The PCR conditions were initial denaturation (3 min at 95°C), 26 cycles of amplification (20 s at 95°C, 20 s at 48°C, and 30 s at 72°C), and terminal extension (3 min at 72°C). Both the forward and the reverse primers each had an additional, sample-specific 6-bp bar code at the 5′ end that differed by at least 2 bp between samples and contained no homopolymers. The amplicons were quantified photometrically (NanoDrop; Thermo Fisher Scientific, Schwerte, Germany) and mixed in equimolar amounts before further analysis. Adaptor ligation, subsequent amplification, and pyrosequencing (454 GS FLX Titanium; Roche, Mannheim, Germany) were done by a commercial service (GATC Biotech; Konstanz, Germany).

Sequence processing and classification. Pyrotag data were preprocessed using the mothur software suite (version 1.15.0) (59), following the strategy described by Schloss et al. (58), with slight modifications. After sorting the sequences by their unique bar codes, all sequences that were shorter than 200 bp, contained ambiguous bases, had errors in the primer sequence, or showed homopolymer regions of more than 10 nucleotides were removed from the data sets. For phylotype analyses, the remaining sequences were denoised as previously described (58); for classification analyses, the sequences were aligned against the SILVA 102 nonredundant database (53) using a stand-alone version of the SINA aligner (http://www.arb-silva.de).

The sequences were assigned to taxonomic groups with the naïve Bayesian classifier implemented in the mothur software using a manually curated reference database and a confidence threshold of 60%. The reference database consisted of the SILVA 102 nonredundant database amended with numerous unpublished sequences from termite and cockroach guts obtained in our laboratory in Marburg. The existing classification of the SILVA database was extended and refined down to the genus level by introducing additional, termite-specific groups and renaming redundant or uninformative taxa. To allow processing in the mothur software environment and to improve the speed of the classifier, uninformative sequences from those taxa that contained no gut-related sequences were removed. The resulting reference database (82,400 sequences) contained all bacterial isolates, all uncultivated bacteria from intestinal environments, and at least three representative sequences from every other lowest-level group in the SILVA database. It is available from the authors upon request.

RESULTS

Physicochemical gut conditions. Microsensor profiles along the gut axis of *N. corniger* showed strong dynamics of oxygen concentration (Fig. 2A). Total anoxia was observed in the highly dilated hindgut paunch (anterior P3 compartment) but not in the less dilated, posterior part of the P3 compartment, where traces of oxygen at its center were often found, which suggested that a complete removal of oxygen depends on the diameter of the respective gut region. Radial oxygen profiles of the P3 compartment showed that the gut periphery acts as an oxygen sink, with the microoxic

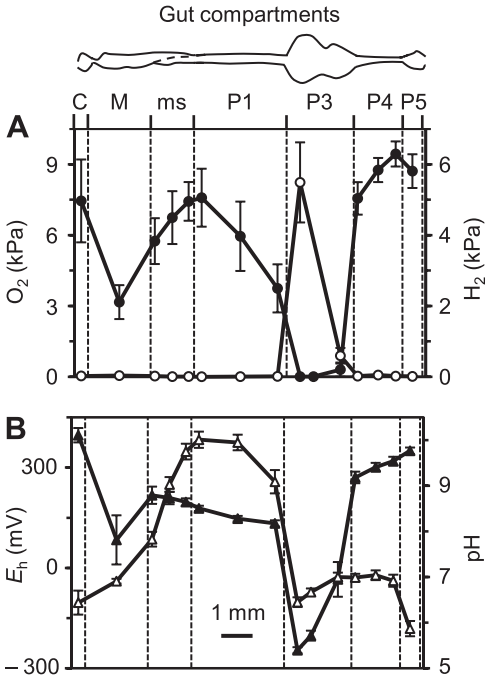

FIG 2 Axial profiles of oxygen (●) and hydrogen (○) partial pressure (A) and of redox potential (▲) and pH (△) (B) along the gut of *Nasutitermes corniger*, measured at the gut center. Values are means ± standard errors obtained with 8 to 12 termites (except for the crop, which was lost in about half of the preparations). For definitions of the abbreviations of the gut compartments, see the legend to Fig. 1.

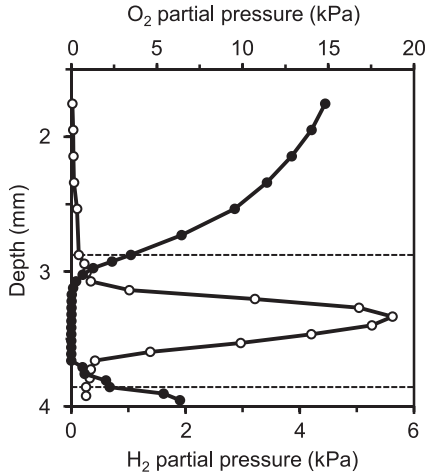

FIG 3 Radial profiles of oxygen (●) and hydrogen (○) partial pressure in the agarose-embedded anterior P3 compartment of *Nasutitermes corniger* relative to the agarose surface. The dotted lines indicate the positions of the proximal and distal gut wall. The profiles were selected as being typical among six similar sets obtained with different termites.

zone typically extending 200 to 300 μm below the gut wall (Fig. 3). However, the penetration depth of oxygen changed with the depth of embedding. If the agarose layer above the hindgut paunch was very shallow (<2 mm), the entire compartment occasionally became oxic.

The oxygen status corresponded to the redox conditions in the respective compartments; i.e., only the anoxic region (P3) had a negative redox potential (Fig. 2B). The accumulation of H_2 was also restricted to the P3 compartment, with maximal values occurring in the anterior region (Fig. 2A). Radial hydrogen profiles of the anterior P3 compartment revealed steep H_2 gradients from the gut center toward the gut wall (Fig. 3). However, hydrogen partial pressures in P3 varied over a wide range (from 0.02 to 12 kPa) and were quite sensitive to the depth of embedding. When intestinal hydrogen partial pressures were measured *in situ* (by inserting the microsensor through the dorsal cuticle into the abdomen of decapitated termites), hydrogen partial pressures ranged from 0.1 to 2.4 kPa. However, these values have to be regarded with caution, because the intransparency of the cuticle did not allow us to determine the exact location of the microsensor tip or to assess the damage to the intestines caused by the sensor.

The pH of the gut contents was also found to be highly dynamic along the gut axis. The intestinal pH was slightly acidic in the crop, was circumneutral in the midgut, and increased sharply in the mixed segment. The most alkaline values (pH 9.3 to 10.9) were found in the anterior P1 compartment. The pH decreased again in the P3 compartment, remained neutral in most of the posterior hindgut, and again turned slightly acidic in the P5 compartment (Fig. 2B).

Metabolite pools. The metabolites accumulating in the different gut sections of *N. corniger* were determined by means of HPLC and GC (Table 1). Acetate was the predominant metabolite in all gut sections, except for the midgut, where succinate was more abundant. The highest proportion of acetate was present in the P3 section, which also contained the largest metabolite pool of all compartments. Lactate was detected only in the posterior gut, with the highest concentration being in the P5 section. Similar results have been previously reported for other *Nasutitermes* spp., except that the pool sizes of propionate, butyrate, and formate were smaller (66).

Bacterial diversity. The microbial cell counts in homogenates of individual gut sections of *N. corniger* differed greatly (Table 1). The highest absolute number was found in the P3 compartment (1.5×10^7 cells), surpassing those in the other gut regions by more than 2 orders of magnitude. The microbiota of the crop consisted mostly of cocci, whereas the midgut microbiota was dominated by short rods; cells with a spirochetal shape were rare in both compartments. In the P1 compartment, we observed mostly longer rods; cocci were less abundant, and the density of cells with a spirochetal shape began to increase. The density of spirochetes was highest in the P3 compartment but decreased again in the posterior sections, whose microbiota was dominated by coccoid cells.

Bacterial diversity in the different gut sections of *N. corniger* and in total hindguts of *N. corniger* and *N. takasagoensis* was determined by pyrotag sequencing of the V3-V4 region of the 16S rRNA genes in the DNA extracted from the different samples. Trimming and quality control removed 10 to 20% of the sequences from each data set, resulting in sequence libraries of 3,200 to 26,000 reads per sample (see Table S1 in the supplemental material).

Preliminary analysis using the classifier of the online platform of the Ribosomal Database Project (RDP; release 10) (72) yielded large fractions of unclassified sequences at all taxonomic levels (Table 2). Since most of the unclassified sequences were termite-specific bacterial groups that were not represented or poorly resolved in the reference database used by RDP, we prepared a man-

TABLE 1 Pool sizes of major metabolites, fresh weight, and microbial cell counts for different gut sections of *Nasutitermes corniger*[a]

Section	Pool size (nmol)						Fresh wt (mg)	Cell count (10^6 section^{-1})	Cell density (10^9 g^{-1})[b]
	Acetate	Propionate	Butyrate	Succinate	Lactate	Formate			
Crop	0.7 ± 0.1	0.2 ± 0.2	—[c]	0.4 ± 0.1	—	0.3 ± 0.1	0.7 ± 0.2	0.15 ± 0.03	0.21 ± 0.07
Midgut	0.9 ± 0.0	0.2 ± 0.2	—	2.0 ± 1.0	—	0.1 ± 0.1	0.6 ± 0.1	0.08 ± 0.02	0.13 ± 0.04
ms/P1	1.4 ± 0.2	0.1 ± 0.1	—	1.1 ± 0.7	—	0.7 ± 0.1	0.8 ± 0.2	0.10 ± 0.04	0.13 ± 0.06
P3	8.6 ± 1.8	0.7 ± 0.4	0.1 ± 0.1	1.0 ± 0.8	0.1 ± 0.1	0.5 ± 0.1	1.4 ± 0.3	15.2 ± 3.1	10.9 ± 3.2
P4	2.1 ± 1.0	0.6 ± 0.2	0.1 ± 0.1	0.3 ± 0.1	0.1 ± 0.1	0.7 ± 0.1	0.4 ± 0.2	0.08 ± 0.01	0.20 ± 0.10
P5	1.9 ± 1.2	0.4 ± 0.2	—	0.3 ± 0.2	0.7 ± 0.7	0.6 ± 0.2	0.6 ± 0.5	0.04 ± 0.01	0.07 ± 0.06
Total gut[d]	15.6 ± 2.4	2.2 ± 0.5	0.2 ± 0.2	5.1 ± 1.5	0.9 ± 0.7	2.9 ± 0.3	4.5 ± 0.7	15.6 ± 3.1	3.47 ± 0.87

[a] Values are averages (± mean deviation) for two homogenates of 40 gut sections each.
[b] Based on fresh weight, using error propagation.
[c] —, below detection limit (ca. 0.02 nmol).
[d] Calculated from the amount in each compartment.

ually curated reference database specifically adapted to the bacterial diversity in termite guts (see Materials and Methods). Reclassification of the samples using the mothur software suite (version 1.15.0) (59) resulted in a significantly improved classification at the phylum level, reducing the fraction of unclassified sequences in the different samples from 4 to 22% to 1 to 2%. The effect was even stronger at lower taxonomic ranks; at the genus level, the fraction of unclassified sequences in the samples decreased from 43 to 90% to 11 to 33%. The remaining sequences could be assigned only to higher taxa, mostly because closely related reference sequences were lacking. Closer inspection of 36 randomly selected sequences without phylum-level classification revealed that half of them were putative chimeras and the other half did not code for 16S rRNA.

The individual gut sections of *N. corniger* each contained sequences from 200 to 300 different taxa (genus level), with the highest numbers being found in the crop, P3, and P4 (Table 3). Similarity-based clustering of the sequences into phylotypes with 5% (genus level) or 3% (species level) sequence divergence indicated that the genus/species richness in each sample was considerably higher than that indicated by hierarchical classification (many rare species were not classified in lieu of appropriate reference sequences); predictions of species richness based on the abundance of singletons in the different data sets (using the Chao1 estimator) were higher (Table 3).

Diversity and evenness of the bacterial community were lowest in the midgut, which harbored a few very abundant groups. In the other gut sections, diversity was much higher and community structure was more balanced (Table 3); the same trends were also observed with similarity-based classification (5% cutoff) and hierarchical classification (genus level; details not shown). The relatively small number of phylotypes agrees with the results of Engelbrektson et al. (20), who observed less than 1,000 phylotypes in their rarefaction analyses when they tested several primer pairs for pyrotag sequencing using *N. corniger* luminal P3 hindgut compartment DNA as the template. Nevertheless, the composition of the communities differed substantially between the compartments (Table 4). High similarities were observed between the crop and hindgut (P4 and P5), whereas the midgut had only low similarities to other compartments.

Community structure. The major bacterial phyla consistently encountered in the different gut compartments of *N. corniger* were *Spirochaetes*, candidate phylum TG3, *Firmicutes*, *Fibrobacteres*, *Bacteroidetes*, *Proteobacteria*, and *Actinobacteria* (Fig. 4). *Spirochaetes* and members of the TG3 phylum were represented in all compartments but were most abundant in the hindgut paunch (P3). The phylum-level patterns in the posterior hindgut sections (P4 and P5) were similar to the pattern in the crop, except for an increased abundance of *Firmicutes* in all anterior sections.

At higher taxonomic resolution, it becomes apparent that most phyla are represented by various lineages that are often unevenly

TABLE 2 Comparison of classification success at different taxonomic levels using the RDP online platform (release 10) and the curated reference database (this study)

Section	%[a]					
	Phylum		Family		Genus	
	RDP	This study	RDP	This study	RDP	This study
Crop	89	98	79	90	49	76
Midgut	96	99	17	95	10	89
ms/P1	88	98	88	80	46	67
P3	78	99	80	95	57	87
P4	85	99	76	83	46	72
P5	88	99	80	79	45	72

[a] Values are based on the total number of sequences in the sample.

TABLE 3 Diversity and evenness of the bacterial communities in the different gut sections of *Nasutitermes corniger*[a]

Section	No. of genus-level taxa[b]	No. of phylotypes		Diversity index[c]		
		5%	3%	Expected phylotypes[d]	Diversity[e]	Evenness[f]
Crop	298	351	563	1,174	3.39	0.45
Midgut	217	285	511	1,231	1.54	0.20
ms/P1	187	195	337	944	2.80	0.38
P3	264	360	653	1,626	2.42	0.31
P4	307	411	726	1,748	3.87	0.50
P5	173	167	275	494	3.77	0.57

[a] The number of taxa (hierarchical classification to genus level) is compared to the number of phylotypes (similarity-based classification, using a 3% or 5% dissimilarity threshold).
[b] Lowest level of classification.
[c] Diversity indices are based on 3% dissimilarity.
[d] Chao1 estimator (14).
[e] Nonparametric Shannon index (15).
[f] Evenness was calculated as described elsewhere (34).

TABLE 4 Similarity indices of the bacterial communities in different gut sections of *Nasutitermes corniger*

Section	Similarity index[a]					
	Crop	Midgut	P1	P3	P4	P5
Crop	1.00					
Midgut	0.21	1.00				
ms/P1	0.39	0.22	1.00			
P3	0.36	0.13	0.23	1.00		
P4	0.39	0.14	0.33	0.48	1.00	
P5	0.35	0.17	0.33	0.20	0.20	1.00

[a] Bray-Curtis coefficient (8), based on sequence similarity (3% dissimilarity threshold for phylotypes).

distributed among the compartments. Figure 5 summarizes the relative abundance of the 50 major families represented in the different samples; detailed results for all taxonomic ranks can be found in interactive Table S1 in the supplemental material. A prominent example is the *Firmicutes*. In the midgut, most of the sequences of this phylum (80% of all sequences) are members of the order *Clostridiales*, consisting almost exclusively of a particular group of *Lachnospiraceae* (uncultured 67; see Table S1 in the supplemental material). Although this group was also present in the other compartments, it is outnumbered by other *Clostridiales* (*Ruminococcaceae* or family XIII *incertae sedis*) in the posterior hindgut (P4) and by *Lactobacillales* in the crop (here, mainly *Streptococcaceae*) and in the anterior hindgut (P1; here, mainly members of the insect group PeH08 and other, unclassified *Lactobacillales*). Many family-level taxa are highly represented in all gut sections (e.g., the termite clusters in *Fibrobacteres* and TG3 subphylum 1 or some *Bacteroidetes*). In some cases, the patterns in the posterior hindgut sections (P4 and P5) were similar to those of the crop, e.g., the *Ruminococcaceae* (*Clostridiales*), the *Acidobacteriaceae* (*Acidobacteria*), and the candidate divisions OP11, SR1, and TM7.

Many of the sequences obtained from the gut of *N. corniger* represent termite-specific lineages that have already been encountered in clone-based inventories of the gut microbiota of other *Nasutitermes* species (e.g., see references 26, 71, and 73). However, deep sequencing of the communities in the individual gut regions also revealed the presence of many lineages hitherto undetected in termite guts (e.g., from the phyla *Lentisphaerae*, *Planctomycetes*, and *Firmicutes* and candidate divisions OP11, TM7, and SR1), which underlines the high diversity of the gut microbiota also reflected by the high Shannon indices for most compartments (Table 3). Although 75% of the families detected each represent less than 1% of the sequences obtained from the different sections (see Table S1 in the supplemental material), many of these groups are numerically important because of the high density of the community (i.e., in the P3 compartment; Fig. 4) or because of their apparent specificity for termite guts. In any case, it should be considered that, especially in the P3 section, taxa that are close to the detection limit of the pyrotag analysis still form substantial populations.

Interspecific variation. The bacterial community profiles of the P3 compartment are virtually identical to the artificial profiles for the hindgut and whole gut generated using cell density and the relative abundance of different families in the individual compart-

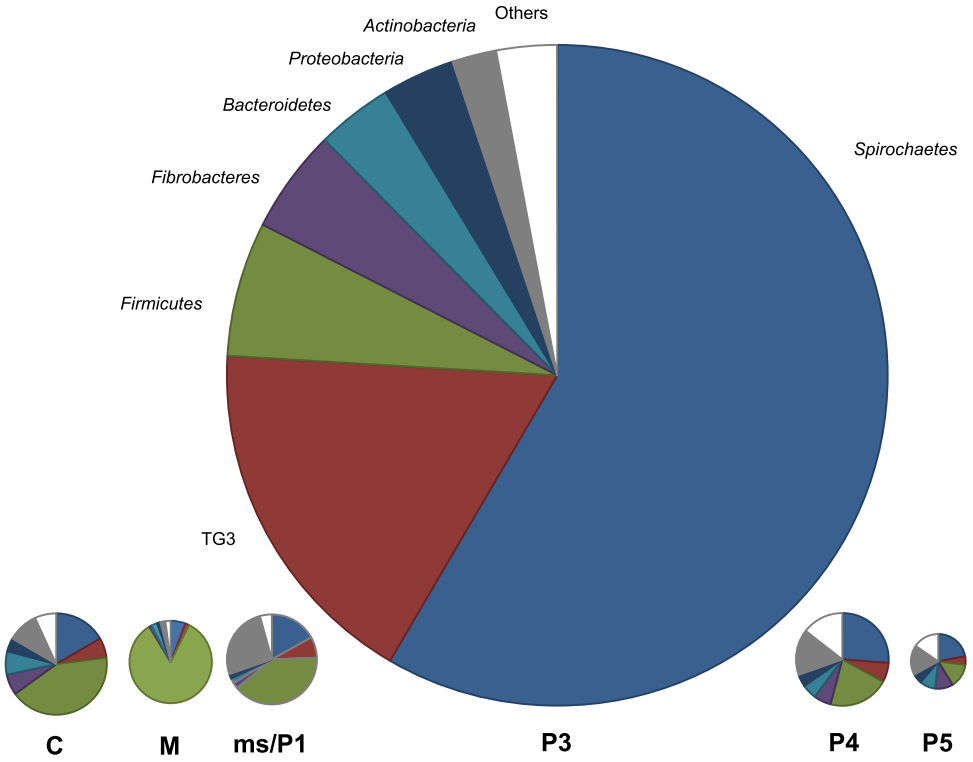

FIG 4 Relative abundance of major bacterial phyla in the different gut compartments of *Nasutitermes corniger*, based on pyrotag analysis of the V3-V4 region of the 16S rRNA genes. The area of the circles reflects the microbial cell counts in the respective gut sections (Table 1). For definitions of the abbreviations, see the legend to Fig. 1.

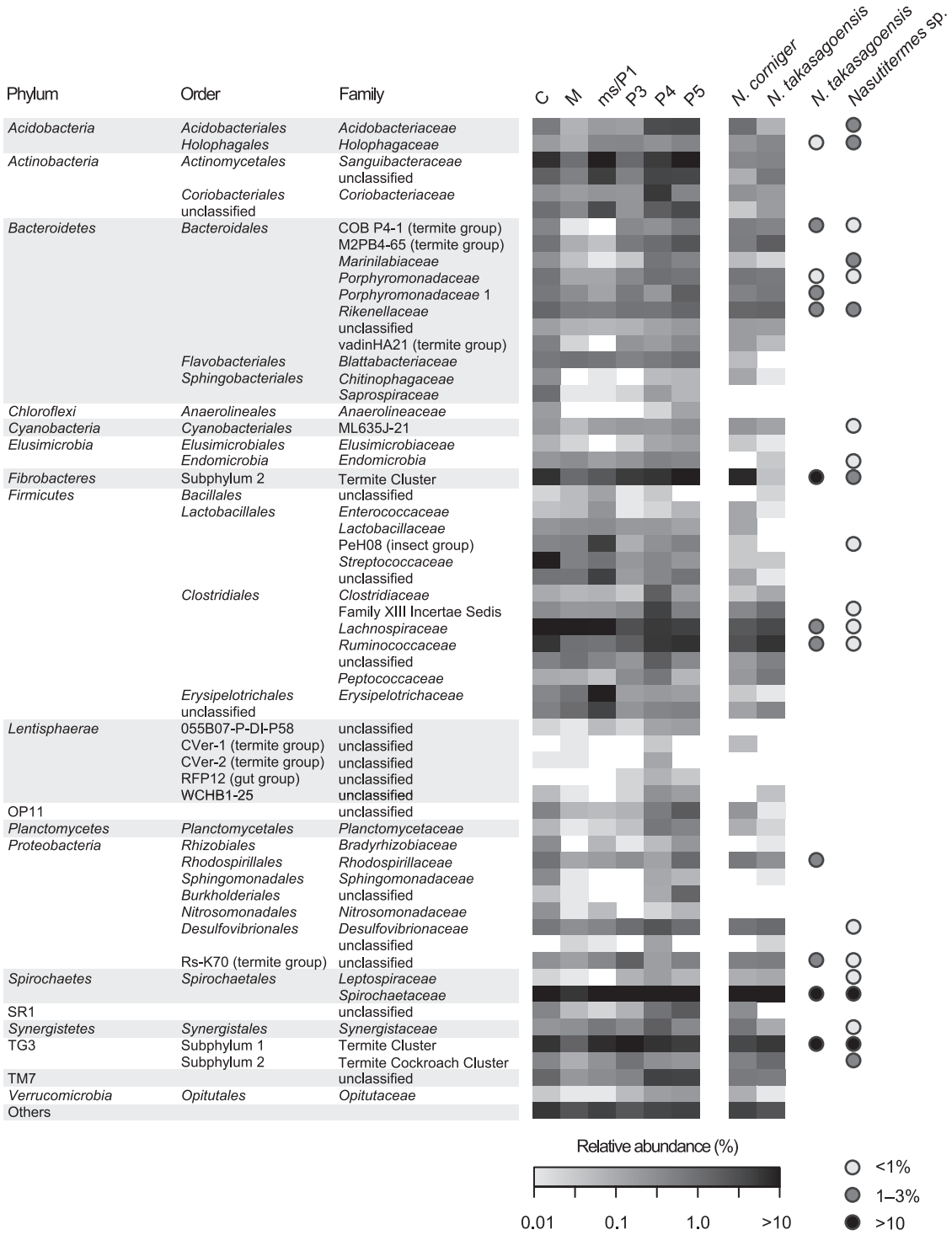

FIG 5 Relative abundance of the major bacterial taxa in the different gut sections of *Nasutitermes corniger* (for definitions of the abbreviations, see the legend to Fig. 1) and in the total hindguts of *N. corniger* and *N. takasagoensis*. Classification is shown down to the family level (for genus level, see Table S1 in the supplemental material). The heat map uses a logarithmic scale to increase the visibility of low-abundance groups. The remaining sequences were extremely diverse (111 to 157 families), but each represented less than 1% of the community in the respective compartment (see Table S1 in the supplemental material). The families represented in previously published clone libraries of *N. takasagoensis* (26) (total gut) and a *Nasutitermes* sp. (73) (P3 lumen) are shown for comparison (shading of circles indicates relative abundance).

ments (see Fig. S2 in the supplemental material), which illustrates that the community profiles of the total gut will always be dominated by the microbiota of the P3 compartment (Fig. 4). At the family level, these profiles were highly similar to replicate profiles of the hindgut and total gut of *N. corniger* (see Fig. S2), which were obtained with different batches of termites from the same nest. At the genus level, only 31% of the classified genera were shared among the profiles, but these genera represented 95% of the total

sequence abundance. This documents the reproducibility of the profiles and the noise in the low-abundance taxa/singletons that leads to high species richness estimations (Table 3). The differences between the samples were exclusively in the low-abundance taxa. The similarities between the hindgut profiles of *N. corniger* and the closely related *N. takasagoensis*, an allopatric species from Japan, were slightly lower (23% shared genera), but the profiles showed striking similarities in the presence and abundance of family-level taxa (Fig. 5).

Comparison to clone libraries. A comparison of the pyrotag data sets of *N. corniger* and *N. takasagoensis* to previous clone libraries of the bacterial 16S rRNA genes from the gut of *Nasutitermes* species showed that each of the major family-level lineages is represented in all *Nasutitermes* species, although their relative abundance differs (Fig. 5). A notable exception is a termite-specific lineage of *Bacteroidetes* (M2PB4-65) that is moderately abundant in the 454 data sets (0.6 to 1.7%) but not represented in the clone libraries. Strong differences between the data sets are encountered among the *Fibrobacteres*, TG3, *Firmicutes*, and *Spirochaetes*, particularly in the virtual absence of *Fibrobacteres* from the hindgut of the batch of *N. takasagoensis* used in this study.

When we compared at the genus level the bacteria in the total P3 section of *N. corniger* to the bacteria detected in the lumen of this compartment of a *Nasutitermes* sp. collected in Costa Rica (73), we found that 79% of the taxa in the pyrotag libraries were represented, which indicated that the bulk of the P3 compartment gut microbiota was already detected by a clone library of 1,252 sequences (73). However, the pyrotag library of P3 (24,029 reads) comprised 217 additional taxa. Many of them were also present in the pyrotag library of *N. takasagoensis*, which indicated that they are likely to occur also in other *Nasutitermes* species.

An interesting aspect became apparent when we compared the two data sets in the opposite direction. Since the pyrotag data set for *N. corniger* generated in this study was obtained from a homogenate of the complete P3 compartment and the clone library of *Nasutitermes* sp. was based only on its luminal content (73), any major taxa present in the analysis of the total compartment but missing from the luminal sample potentially represent wall-associated bacteria. To compensate for the lower sequencing depth of the luminal sample, a threshold for the larger amounts of pyrotag sequences was set by taking the noise signal (i.e., one sequence) multiplied by 3 (i.e., three sequences in the luminal data set corresponding to 0.24% in the pyrotag data set). Taking this threshold, we discovered 10 taxa that are strong candidates for gut wall-associated bacteria (see Table S1 in the supplemental material), including *Sanguibacter* spp. and other *Actinobacteria*, *Bacteroidetes* cluster V (*Porphyromonadaceae* 1), *Arthromitus* spp. (*Lachnospiraceae*), and some lineages of *Spirochaetaceae* specific for termite guts. Together, they formed 10% of the sequences from the P3 compartment. In contrast, taxa that were exclusively present in the luminal sample (see Table S1 in the supplemental material) were only a small fraction (0.6%) of the clones in the library. Moreover, two of these groups, OPB56 (*Chlorobi*) and Rs-H88 (*Spirochaetes*), were present in the total hindgut sample of *N. corniger*.

DISCUSSION

This is the first comprehensive analysis of the digestive tract of a wood-feeding higher termite from a microbiological perspective. It combines a microsensor study of physicochemical gut conditions with a highly resolved analysis of the bacterial microbiota in the individual gut compartments. The results revealed that the gut is a highly structured microenvironment, with differences in metabolic activities and microbial community structure. The dilated hindgut paunch (P3) contains the bulk of the microbiota, but other compartments, such as the alkaline P1 and the tubular P4, also harbor smaller communities distinct from those in other gut regions. The differences are already apparent at the phylum level, and a detailed analysis of relative abundance indicates that individual lineages preferentially colonize particular niches. The results allow us to draw cautious conclusions concerning the functions of particular bacterial lineages in the respective sections.

Hindgut paunch. Since higher termites lack cellulolytic flagellates, wood fiber in the dilated hindgut paunch has to be digested by a purely prokaryotic microbiota (13). The hindgut of *Nasutitermes takasagoensis* and *N. walkeri* contains substantial cellulolytic activity (70), and metagenomic analysis of the luminal contents of the P3 compartment of another *Nasutitermes* species has identified numerous glycosyl hydrolases putatively involved in the degradation of cellulose and hemicelluloses. The genes have tentatively been assigned to members of the phyla *Fibrobacteres* and *Spirochaetes* on the basis of phylogenetic binning (73). Diverse members of these phyla and of the related TG3 phylum (included in the *Fibrobacteres* by Warnecke and colleagues [73]) have been documented to occur abundantly in the hindgut of *Nasutitermes* species (17, 48, 46, 26, 73). In accordance with these reports, the mentioned phyla were also highly represented in the pyrotag sequences of the total hindgut of *N. corniger* and *N. takasagoensis*. They dominate the microbiota in the P3 compartment of *N. corniger* (Fig. 4), the major microbial bioreactor in terms of anoxic status, microbial cell count, and concentration of fermentation products.

Interestingly, the P3 compartment is also the only gut region where H_2 accumulated. Hydrogen partial pressures in the anterior P3 of *N. corniger* were in the same range as those in the paunch of *Reticulitermes flavipes* (18), where H_2 production is largely attributed to the gut flagellates. Several higher termites, including *Nasutitermes triodiae*, have been reported to emit H_2 *in vivo* (65), but microsensor profiles have so far been available only for soil-feeding *Cubitermes* spp., where the mixed segment and the P3 showed substantial accumulation of H_2 (60). The bacterial populations responsible for hydrogen production have not been identified, but by means of phylogenetic analyses of conserved single-copy protein-coding genes, Warnecke et al. (73) could link the iron-only hydrogenases in the metagenome of a *Nasutitermes* sp. to members of the *Spirochaetes*. Molecular hydrogen is a major fermentation product of carbohydrates in many *Spirochaeta* spp. (35) and also in *Treponema azotonutricium*, an isolate from the lower termite *Zootermopsis angusticollis* (24). All isolates of termite gut treponemes possess several [FeFe] hydrogenases (2), and related hydrogenase genes are also present in other lower termites (1). It is therefore likely that spirochetes are—at least in part—also responsible for hydrogen production in *Nasutitermes* spp. It is possible that members of the *Fibrobacteres* and TG3, the other highly abundant bacterial phyla in the P3 compartment of *N. corniger* and hindguts of other *Nasutitermes* spp., also contribute to hydrogen production. While nothing is known about these uncultivated lineages, the genome of the distantly related *Fibrobacter succinogenes* does not encode any hydrogenases (64), and there were no

hydrogenases binning with *Fibrobacteres* in the *Nasutitermes* sp. metagenome (73).

The steep radial profiles of H_2 in the P3 compartment of *N. corniger* indicate the presence of a strong hydrogen sink, which is in agreement with the high rates of reductive acetogenesis in hindgut homogenates of several *Nasutitermes* species (7) and consolidates the accumulation of large amounts of H_2 within the lumen of the hindgut paunch with the low rates of hydrogen emission by living termites (65). Analyses of the *fhs* gene, encoding formyltetrahydrofolate synthetase (FTHFS), a functional marker for the Wood-Ljungdahl pathway, have provided strong evidence that spirochetes are responsible for reductive acetogenesis from H_2 and CO_2 in the gut of lower termites (e.g., see references 32, 47, 51, and 55). A metagenomic survey of the hindgut microbiota of a *Nasutitermes* sp. has indicated that *fhs* genes in the hindgut community are highly similar to those in the hindgut of lower termites, including that of the genuine homoacetogen *Treponema primitia* (73). The *cooS* genes in the metagenome, encoding a catalytic subunit of the carbon monoxide dehydrogenase, have also been predicted to be encoded by treponemes (73).

It is not clear whether all spirochetal lineages present in the *Nasutitermes* gut are involved in reductive acetogenesis. Furthermore, not all *fhs* genes obtained by Warnecke et al. (73) are clustered with treponemal sequences. It is possible that members of the *Ruminococcaceae* (Fig. 5) also contribute to reductive acetogenesis in the hindgut because many *Ruminococcus* species are homoacetogenic (33, 54). The same argument can be made for the *Holophagaceae* (*Acidobacteria*; Fig. 5) present in all gut compartments of *N. corniger* and the hindgut sample of *N. takasagoensis*, which are closely related to the homoacetogenic *Holophaga foetida* (37).

In view of the large surface-to-volume ratios of small guts (10), the gut wall emerges as an important microhabitat. Methanogenic archaea associated with the gut wall of lower termites have been implicated as a hydrogen sink, both in methanogenesis and owing to their capacity for hydrogen-dependent reduction of inflowing oxygen (67). However, methanogenesis is not as important in *Nasutitermes* spp. as in other termite species (see reference 11 and references therein). The situation is a bit more ambiguous in the case of sulfate-reducing microorganisms. About 1% of the sequences in the P3 compartment (*Desulfovibrio* 1; see Table S1 in the supplemental material) represent sulfate-reducing *Deltaproteobacteria* related to *Desulfovibrio intestinalis*, which—like other *Desulfovibrio* spp. isolated from termite guts—exhibits high rates of hydrogen-dependent oxygen reduction (22, 31). However, it is not known whether the *Desulfovibrio* spp. in *Nasutitermes* are located at the hindgut wall.

Clearly, the radial organization of the microbiota and the location of individual populations with respect to the oxygen gradient are important issues. Although the 454 data sets of the gut sections do not contain direct information about the localization of microorganisms within the respective compartments, the obvious absence of some bacterial groups from the purely luminal sample of the P3 gut compartment (73) compared to the total P3 sample allows us to make some careful inferences regarding peripheral localization. Among the possible gut wall colonizers are populations of the genus *Sanguibacter*, a genus comprising aerobic and facultatively anaerobic isolates (e.g., see reference 28), and other unclassified lineages of *Actinobacteria*. Several lineages of *Trinervitermes* cluster A and several other termite-specific *Spirochaetaceae* groups (see Table S1 in the supplemental material) are also abundant in the total P3 sample of *N. corniger* but absent from the luminal sample of a *Nasutitermes* sp. (73), which is in accordance with previous reports of an attachment of spirochetes to the gut wall of lower and higher termites (17, 41). An association with the gut wall of many lower termites has also been documented for relatives of the *Bacteroidales* cluster V (42), a group that is also abundantly encountered in gut homogenates of *Nasutitermes* spp. (26; this study). The frequent association of cluster V *Bacteroidales* also with the surface of cellulolytic protists in lower termites (43) suggests that the need for attachment is a strategy to prevent washout. The presence of oxygen-removing mechanisms among obligate anaerobes, necessary for the colonization of the microoxic gut periphery, has been previously documented for *Methanobrevibacter* species in lower termites (67) and is also encountered among the *Bacteroidales* (3).

Posterior hindgut. Microbial cell counts decrease by 2 orders of magnitude and cell density drops 50-fold between the P3 and P4 section (Table 1), which suggests that the microbial biomass produced in P3 is digested after being transported into the posterior hindgut with the flow of the digesta. The distinct difference in community structure between the P3 and P4 sections (Fig. 5) indicates the presence of a microbiota specifically adapted to the environment of the posterior hindgut. Most obvious is the increase in relative abundance of *Acidobacteriaceae* and *Coriobacteriaceae* (see Table S1 in the supplemental material), but also, specific lineages of *Lentisphaerae* and members of candidate divisions OP11, SR1, and TM7 are enriched in the posterior hindgut. Distinct changes in diversity and community structure have also been observed between the alkaline P3 and the neutral P4 compartments of soil-feeding *Cubitermes* spp. (61, 62). Since both gut regions are neutral in *Nasutitermes* spp. (9; this study), it is likely that factors other than pH are responsible for this shift. Rather, the force driving community structure could be the increasing influence of oxygen in the tubular P4 section. The slightly acidic pH of the P5 compartment observed in *N. corniger* has also been found among several soil-feeding species (pH 5 to 6) (12).

Crop and midgut. Since sound wood is a highly nitrogen-deficient diet, termites have developed the strategy to exploit the assimilatory capacities of their gut microbiota to acquire essential amino acids and vitamins (13). This is accomplished by digesting microbial biomass derived from the hindgut contents—either by coprophagy or by proctodeal trophallaxis. Although little is known about the behavior of *Nasutitermes* species, numerous similarities in the community patterns of the rectum (P5) and the anterior gut (crop) suggest that fecal material is consumed by the termites (Fig. 5). This agrees with observations of proctodeal feeding in *N. corniger* and other species (R.H.S., unpublished data). The strong shift in the bacterial community profiles (Fig. 5) and the reduction of microbial density between crop and midgut indicate that bacteria are digested in the midgut, which is in agreement with the presence of lysozyme and protease activities in this gut region (23). The community of the midgut is dominated by *Firmicutes*, particularly members of *Lachnospiraceae* (Fig. 5), which represent a lineage of uncultivated bacteria from intestinal environments, including termite guts (uncultured 67 group; see Table S1 in the supplemental material). The family *Lachnospiraceae* comprises many species with high proteolytic, xylanolytic, and also cellulolytic activities (e.g., *Butyrivibrio* and *Pseudobutyrivibrio* spp.) (16), but it remains to be clarified whether

these bacteria contribute to the digestive capacities of the midgut of *Nasutitermes* spp. (69) or whether they are simply transient and inactive forms (e.g., spores) of bacteria residing in other gut regions.

Alkaline gut regions. The anterior hindgut of many higher termites is highly alkaline (5). In soil-feeding Termitinae, the pH increases sharply in the mixed segment and reaches its maximum (pH > 12) in the P1 compartment (12). The alkalinity in the tubular P1 of *N. corniger* is considerably less pronounced (pH 10), and the pH already returns to neutral in P3, a compartment that remains strongly alkaline in the soil feeders. Since the profiles obtained for *N. corniger* (this study) were almost identical to previous profiles of *N. nigriceps* (9), it seems safe to conclude that they are typical, at least for the wood-feeding members of this genus.

A prevalent bacterial lineage in the alkaline P1 section of *N. corniger* is the genus *Turicibacter* (*Firmicutes*, *Erysipelotrichaceae*; abundance, 13%; see Table S1 in the supplemental material); their relative abundance in all other compartments is less than 1%. Representatives of this cluster have also been detected in the (putatively) alkaline P1 regions of the soil-feeding *Pericapritermes latignathus* and a grass-feeding *Speculitermes* sp. (68) and in the alkaline midgut of the humivorous larva of the scarab beetle *Pachnoda ephippiata* (19), which indicates an adaptation to high pH. The occurrence of *Turicibacter* spp. in the gut of a *Microcerotermes* sp. (27), which also comprises an alkaline P1 (9), is in agreement with this assumption. However, alkaliphily is not a typical trait for the whole genus; the next cultured relative, *Turicibacter sanguinis*, does not grow above pH 8 (6), and members of the *Turicibacter* clade are also present in mammals (36), which lack a highly alkaline gut.

Other bacterial groups prevailing in the P1 section are several lineages of *Lactobacillales* (*Firmicutes*). Sequences of cluster PeH08 (5% relative abundance) have been obtained from the alkaline compartments of other higher termites (68) and beetle larvae (19) but were also encountered in the posterior hindgut compartments of *N. corniger* (Fig. 5; see Table S1 in the supplemental material). The P1 section also contains a small number of sequences (1%) from a termite-specific lineage of *Lachnospiraceae* that is related to the sequences NT-1 and NT-2, which have previously been assigned to rod-shaped bacteria predominantly colonizing the mixed segment of *N. takasagoensis* (71). The presence of these bacteria in this sample is explained by the inclusion of the mixed segment in the P1 section, which was not separated for technical reasons.

Pyrotag sequencing of termite gut microbiota. The diversity and community structure of the bacterial gut microbiota of termites have been addressed by numerous studies (see reference 45). Many of the more detailed analyses combined Sanger sequencing of 16S rRNA genes with terminal restriction fragment length polymorphism (T-RFLP) profiling, thus compensating for the shortcomings of the individual approaches (Sanger sequencing is notoriously undersampled, and T-RFLP analyses lack phylogenetic resolution). The application of high-throughput sequencing techniques in targeting the 16S rRNA gene opened a new dimension in microbial ecology studies, allowing the detection of as-yet-undetected microorganisms of very low abundance (63).

As in all PCR-based approaches, primer bias is an important issue. Our pyrotag sequencing data provided a good coverage of all lineages previously discovered by Sanger sequencing (73), which documented that the primers for the V3-V4 region did not introduce a serious bias over the 27F-1492R primers. The striking difference in the abundance of *Fibrobacteres* sequences between the clone library (26) and pyrotag library (this study) of *N. takasagoensis* (Fig. 5) may be rooted in the different batches of termites used in the respective studies.

The results of our study underline the suggestion that a comprehensive and well-curated database is crucial for a reliable sequence assignment (75). Refining the classification of the SILVA database by the introduction of additional, termite-specific groups significantly improved the assignment of pyrotag reads, especially at lower taxonomic levels (Table 2). This revealed the presence of rare taxa that were not discovered in previous, clone-based studies of *Nasutitermes* spp. An example are the sequences related to the fat-body-colonizing *Blattabacterium* (*Flavobacteria*, 0.5 to 0.9% relative abundance), which so far has been detected only in cockroaches and the primitive termite *Mastotermes darwiniensis* (38) and whose presence in higher termites requires further analysis.

The high resolution and fast sample treatment using pyrotag sequencing provide perfect tools for community profiling, combining the virtues of fingerprinting approaches with the benefit of exact taxonomic classification. The large sampling depths of pyrotag sequencing also decrease the detection limit of the analysis, which will help to investigate the existence of a core microbiota and other important questions concerning the evolution of the termite gut microbiota from a putative dictyopteran ancestor.

ACKNOWLEDGMENTS

This study was supported by the Max Planck Society. Tim Köhler received a doctoral fellowship from the International Max Planck Research School for Environmental, Cellular, and Molecular Microbiology.

We thank Gaku Tokuda for providing termites and Yuichi Hongoh and Moriya Ohkuma for sharing unpublished details of a previous study.

REFERENCES

1. **Ballor NR, Leadbetter JR.** 2012. Analysis of extensive [FeFe] hydrogenase gene diversity within the gut microbiota of insects representing five families of *Dictyoptera.* Microb. Ecol. **63**:586–595.
2. **Ballor NR, Paulsen I, Leadbetter JR.** 2012. Genomic analysis reveals multiple [FeFe] hydrogenases and hydrogen sensors encoded by treponemes from the H_2-rich termite gut. Microb. Ecol. **63**:282–294.
3. **Baughn AD, Malamy MH.** 2004. The strict anaerobe *Bacteroides fragilis* grows in and benefits from nanomolar concentrations of oxygen. Nature **427**:441–444.
4. **Bignell DE.** 2011. Morphology, physiology, biochemistry and functional design of the termite gut: an evolutionary wonderland, p 375–412. *In* Bignell DE, Roisin Y, Lo N (ed), Biology of termites: a modern synthesis. Springer, Dordrecht, Netherlands.
5. **Bignell DE, Eggleton P.** 1995. On the elevated intestinal pH of higher termites (Isoptera: Termitidae). Insect Soc. **42**:57–69.
6. **Bosshard PP, Zbinden R, Altwegg M.** 2002. *Turicibacter sanguinis* gen. nov., sp. nov., a novel anaerobic, Gram-positive bacterium. Int. J. Syst. Evol. Microbiol. **52**:1263–1266.
7. **Brauman A, Kane MD, Labat M, Breznak JA.** 1992. Genesis of acetate and methane by gut bacteria of nutritionally diverse termites. Science **257**:1384–1387.
8. **Bray JR, Curtis JT.** 1957. An ordination of the upland forest communities of southern Wisconsin. Ecol. Monogr. **27**:325–349.
9. **Brune A, Emerson D, Breznak JA.** 1995. The termite gut microflora as an oxygen sink: microelectrode determination of oxygen and pH gradients in guts of lower and higher termites. Appl. Environ. Microbiol. **61**:2681–2687.
10. **Brune A.** 1998. Termite guts: the world's smallest bioreactors. Trends Biotechnol. **16**:16–21.
11. **Brune A.** 2010. Methanogenesis in the digestive tracts of insects, p 707–

728. *In* Timmis KN (ed), Handbook of hydrocarbon and lipid microbiology, vol 8. Springer, Heidelberg, Germany.
12. **Brune A, Kühl M.** 1996. pH profiles of the extremely alkaline hindguts of soil-feeding termites (Isoptera: Termitidae) determined with microelectrodes. J. Insect Physiol. **42**:1121–1127.
13. **Brune A, Ohkuma M.** 2011. Role of the termite gut microbiota in symbiotic digestion, p 439–475. *In* Bignell DE, Roisin Y, Lo N (ed), Biology of termites: a modern synthesis. Springer, Dordrecht, Netherlands.
14. **Chao A.** 1984. Nonparametric estimation of the number of classes in a population. Scand. J. Stat. **11**:265–270.
15. **Chao A, Shen TJ.** 2003. Nonparametric estimation of Shannon's index of diversity when there are unseen species in sample. Environ. Ecol. Stat. **10**:429–443.
16. **Cotta M, Forster R.** 2006. The family Lachnospiraceae, including the genera *Butyrivibrio*, *Lachnospira* and *Roseburia*, p 1002–1021. *In* Dworkin M, Falkow S, Rosenberg E, Schleifer K-H, Stackebrandt E (ed), The prokaryotes, 3rd ed, vol 4. Springer, New York, NY.
17. **Czolij R, Slaytor M, O'Brien RW.** 1985. Bacterial flora of the mixed segment and the hindgut of the higher termite *Nasutitermes exitiosus* Hill (Termitidae, Nasutitermitinae). Appl. Environ. Microbiol. **49**:1226–1236.
18. **Ebert A, Brune A.** 1997. Hydrogen concentration profiles at the oxic-anoxic interface: a microsensor study of the hindgut of the wood-feeding lower termite *Reticulitermes flavipes* (Kollar). Appl. Environ. Microbiol. **63**:4039–4046.
19. **Egert M, Wagner B, Lemke T, Brune A, Friedrich MW.** 2003. Microbial community structure in midgut and hindgut of the humus-feeding larva of *Pachnoda ephippiata* (Coleoptera: Scarabaeidae). Appl. Environ. Microbiol. **69**:6659–6668.
20. **Engelbrektson A, et al.** 2010. Experimental factors affecting PCR-based estimates of microbial species richness and evenness. Environ. Microbiol. **4**:642–647.
21. **Friedrich MW, Schmitt-Wagner D, Lueders T, Brune A.** 2001. Axial differences in community structure of *Crenarchaeota* and *Euryarchaeota* in the highly compartmentalized gut of the soil-feeding termite *Cubitermes orthognathus.* Appl. Environ. Microbiol. **67**:4880–4890.
22. **Fröhlich J, et al.** 1999. Isolation of *Desulfovibrio intestinalis* sp. nov. from the hindgut of the lower termite *Mastotermes darwiniensis*. Can. J. Microbiol. **45**:145–152.
23. **Fujita A, Abe T.** 2002. Amino acid concentration and distribution of lysozyme and protease activities in the guts of higher termites. Physiol. Entomol. **27**:76–78.
24. **Graber JR, Leadbetter JR, Breznak JA.** 2004. Description of *Treponema azotonutricium* sp. nov. and *Treponema primitia* sp. nov., the first spirochetes isolated from termite guts. Appl. Environ. Microbiol. **70**:1315–1320.
25. **Henckel T, Friedrich M, Conrad R.** 1999. Molecular analyses of the methane-oxidizing microbial community in rice field soil by targeting the genes of the 16S rRNA, particulate methane monooxygenase, and methanol dehydrogenase. Appl. Environ. Microbiol. **65**:1980–1990.
26. **Hongoh Y, et al.** 2006. Phylogenetic diversity, localization and cell morphologies of the candidate phylum TG3 and a subphylum in the phylum *Fibrobacteres*, recently found bacterial groups dominant in termite guts. Appl. Environ. Microbiol. **72**:6780–6788.
27. **Hongoh Y, et al.** 2005. Intra- and interspecific comparisons of bacterial diversity and community structure support coevolution of gut microbiota and termite host. Appl. Environ. Microbiol. **71**:6590–6599.
28. **Huang Y, et al.** 2005. *Sanguibacter marinus* sp. nov., isolated from coastal sediment. Int. J. Syst. Evol. Microbiol. **55**:1755–1758.
29. **Hugenholtz P, Goebel BM.** 2001. The polymerase chain reaction as a tool to investigate microbial diversity in environmental samples, p 31–41. *In* Rochelle PA (ed), Environmental molecular microbiology: protocols and applications. Horizon Press Inc., New York, NY.
30. **Jouquet P, Traoré S, Choosai C, Hartmann C, Bignell D.** 2011. Influence of termites on ecosystem functioning. Ecosystem services provided by termites. Eur. J. Soil Biol. **47**:215–222.
31. **Kuhnigk T, Branke J, Krekeler D, Cypionka H, König H.** 1996. A feasible role of sulfate-reducing bacteria in the termite gut. Syst. Appl. Microbiol. **19**:139–149.
32. **Leadbetter JR, Schmidt TM, Graber JR, Breznak JA.** 1999. Acetogenesis from H_2 plus CO_2 by spirochetes from termite guts. Science **283**:686–689.
33. **Leaphart AB, Lovell CR.** 2001. Recovery and analysis of formyltetrahydrofolate synthetase gene sequences from natural populations of acetogenic bacteria. Appl. Environ. Microbiol. **67**:1392–1395.
34. **Legendre P, Legendre L.** 1998. Numerical ecology, 2nd ed. Elsevier, Amsterdam, Netherlands.
35. **Leschine S, Paster B, Canale-Parola E.** 2006. Free-living saccharolytic spirochetes: the genus *Spirochaeta*, p 195–210. *In* Dworkin M, Falkow S, Rosenberg E, Schleifer K-H, Stackebrandt E (ed) The prokaryotes, 3rd ed, vol 7. Springer, New York, NY.
36. **Ley RE, et al.** 2008. Evolution of mammals and their gut microbes. Science **320**:1647–1651.
37. **Liesack W, Bak F, Kreft JU, Stackebrandt E.** 1994. *Holophaga foetida* gen. nov., sp. nov., a new, homoacetogenic bacterium degrading methoxylated aromatic compounds. Arch. Microbiol. **162**:85–90.
38. **Lo N, Bandi C, Watanabe H, Nalepa C, Beninati T.** 2003. Evidence for co-cladogenesis between diverse dictyopteran lineages and their intracellular endosymbionts. Mol. Biol. Evol. **20**:907–913.
39. **Ludwig W, et al.** 2004. ARB: a software environment for sequence data. Nucleic Acids Res. **32**:1363–1371.
40. **Muyzer G, de Waal EC, Uitterlinden AG.** 1993. Profiling of complex microbial populations by denaturing gradient gel electrophoresis analysis of polymerase chain reaction-amplified genes coding for 16S rRNA. Appl. Environ. Microbiol. **59**:695–700.
41. **Nakajima H, Hongoh Y, Usamib R, Kudo T, Ohkuma M.** 2005. Spatial distribution of bacterial phylotypes in the gut of the termite *Reticulitermes speratus* and the bacterial community colonizing the gut epithelium. FEMS Microbiol. Ecol. **54**:247–255.
42. **Nakajima H, et al.** 2006. Phylogenetic and morphological diversity of *Bacteroidales* members associated with the gut wall of termites. Biosci. Biotechnol. Biochem. **70**:211–218.
43. **Noda S, et al.** 2006. Identification and characterization of ectosymbionts of distinct lineages in *Bacteroidales* attached to flagellated protists in the gut of termites and a wood-feeding cockroach. Environ. Microbiol. **8**:11–20.
44. **Noirot C.** 2001. The gut of termites (Isoptera). Comparative anatomy, systematics, phylogeny. II. Higher termites (Termitidae). Ann. Soc. Entomol. Fr. (N.S.) **37**:431–471.
45. **Ohkuma M, Brune A.** 2011. Diversity, structure, and evolution of the termite gut microbial community, p 413–438. *In* Bignell DE, Roisin Y, Lo N (ed), Biology of termites: a modern synthesis. Springer, Dordrecht, Netherlands.
46. **Ohkuma M, Iida T, Kudo T.** 1999. Phylogenetic relationships of symbiotic spirochetes in the gut of diverse termites. FEMS Microbiol. Lett. **181**:123–129.
47. **Ottesen EA, Leadbetter JR.** 2011. Formyltetrahydrofolate synthetase gene diversity in the guts of higher termites with different diets and lifestyles. Appl. Environ. Microbiol. **77**:3461–3467.
48. **Paster BJ, et al.** 1996. Phylogeny of not-yet-cultured spirochetes from termite guts. Appl. Environ. Microbiol. **62**:347–352.
49. **Pernthaler A, Pernthaler J, Amann R.** 2004. Sensitive multi-color fluorescence *in situ* hybridization for the identification of environmental microorganisms, p 711–726. *In* Kowalchuk GA, de Brujin FJ, Head IM, Akkermans ADL, van Elsas JD (ed), Molecular microbial ecology manual, 2nd ed, vol 1. Kluwer Academic Publishers, Dordrecht, Netherlands.
50. **Pernthaler J, Glöckner FO, Schönhuber W, Amann R.** 2001. Fluorescence *in situ* hybridization with rRNA-targeted oligonucleotide probes, p 207–226. *In* Paul J (ed), Methods in microbiology: marine microbiology, vol 30. Academic Press, London, United Kingdom.
51. **Pester M, Brune A.** 2006. Expression profiles of *fhs* (FTHFS) genes support the hypothesis that spirochaetes dominate reductive acetogenesis in the hindgut of lower termites. Environ. Microbiol. **8**:1261–1270.
52. **Pester M, Brune A.** 2007. Hydrogen is the central free intermediate during lignocellulose degradation by termite gut symbionts. ISME J. **1**:551–565.
53. **Pruesse E, et al.** 2007. SILVA: a comprehensive online resource for quality checked and aligned ribosomal RNA sequence data compatible with ARB. Nucleic Acids Res. **35**:7188–7196.
54. **Rieu-Lesme F, Morvan B, Collins MD, Fonty G, Willems A.** 1996. A new H_2/CO_2-using acetogenic bacterium from the rumen: description of *Ruminococcus schinkii* sp. nov. FEMS Microbiol. Lett. **140**:281–286.
55. **Salmassi TM, Leadbetter JR.** 2003. Molecular aspects of CO_2-reductive acetogenesis in cultivated spirochetes and the gut community of the termite *Zootermopsis angusticollis.* Microbiology **149**:2529–2537.
56. **Scheffrahn RH, Cabrera BJ, Kern WH, Jr, Su N-Y.** 2002. *Nasutitermes*

costalis (Isoptera: Termitidae) in Florida: first record of a non-endemic establishment by a higher termite. Florida Entomol. **85**:273–275.
57. **Scheffrahn RH, Krecek J, Szalanski AL, Austin JW.** 2005. Synonymy of the neotropical arboreal termites *Nasutitermes corniger* and *N. costalis* (Isoptera: Termitidae: Nasutitermitinae), with evidence from morphology, genetics, and biogeography. Ann. Entomol. Soc. Am. **98**:273–281.
58. **Schloss PD, Gevers D, Westcott SL.** 2011. Reducing the effects of PCR amplification and sequencing artifacts on 16S rRNA-based studies. PLoS One **6**:e27310. doi:10.1371/journal.pone.0027310.
59. **Schloss PD, et al.** 2009. Introducing mothur: open-source, platform-independent, community-supported software for describing and comparing microbial communities. Appl. Environ. Microbiol. **75**:7537–7541.
60. **Schmitt-Wagner D, Brune A.** 1999. Hydrogen profiles and localization of methanogenic activities in the highly compartmentalized hindgut of soil-feeding higher termites (*Cubitermes* spp.). Appl. Environ. Microbiol. **65**: 4490–4496.
61. **Schmitt-Wagner D, Friedrich MW, Wagner B, Brune A.** 2003. Phylogenetic diversity, abundance, and axial distribution of bacteria in the intestinal tract of two soil-feeding termites (*Cubitermes* spp.). Appl. Environ. Microbiol. **69**:6007–6017.
62. **Schmitt-Wagner D, Friedrich MW, Wagner B, Brune A.** 2003. Axial dynamics, stability, and interspecies similarity of bacterial community structure in the highly compartmentalized gut of soil-feeding termites (*Cubitermes* spp.). Appl. Environ. Microbiol. **69**:6018–6024.
63. **Sogin ML, et al.** 2006. Microbial diversity in the deep sea and the underexplored "rare biosphere." Proc. Natl. Acad. Sci. U. S. A. **103**:12115–12120.
64. **Suen G, et al.** 2011. The complete genome sequence of *Fibrobacter succinogenes* S85 reveals a cellulolytic and metabolic specialist. PLoS One **6**:e18814. doi:10.1371/journal.pone.0018814.
65. **Sugimoto A, et al.** 1998. Methane and hydrogen production in a termite-symbiont system. Ecol. Res. **13**:241–257.
66. **Tholen A, Brune A.** 2000. Impact of oxygen on metabolic fluxes and *in situ* rates of reductive acetogenesis in the hindgut of the wood-feeding termite *Reticulitermes flavipes.* Environ. Microbiol. **2**:436–449.
67. **Tholen A, Pester M, Brune A.** 2007. Simultaneous methanogenesis and oxygen reduction by *Methanobrevibacter cuticularis* at low oxygen fluxes. FEMS Microbiol. Ecol. **62**:303–312.
68. **Thongaram T, et al.** 2005. Comparison of bacterial communities in the alkaline gut segment among various species of higher termites. Extremophiles **9**:229–238.
69. **Tokuda G, et al.** 2012. Cellulolytic environment in the midgut of the wood-feeding higher termite *Nasutitermes takasagoensis.* J. Insect Physiol. **58**:147–154.
70. **Tokuda G, Watanabe H.** 2007. Hidden cellulases in termites: revision of an old hypothesis. Biol. Lett. **3**:336–339.
71. **Tokuda G, Yamaoka I, Noda H.** 2000. Localization of symbiotic clostridia in the mixed segment of the termite *Nasutitermes takasagoensis* (Shiraki). Appl. Environ. Microbiol. **66**:2199–2207.
72. **Wang Q, Garrity GM, Tiedje JM, Cole JR.** 2007. Naive Bayesian classifier for rapid assignment of rRNA sequences into the new bacterial taxonomy. Appl. Environ. Microbiol. **73**:5261–5267.
73. **Warnecke F, et al.** 2007. Metagenomic and functional analysis of hindgut microbiota of a wood-feeding higher termite. Nature **450**:560–565.
74. **Watanabe H, Tokuda G.** 2010. Cellulolytic systems in insects. Annu. Rev. Entomol. **55**:609–632.
75. **Werner JJ, et al.** 2012. Impact of training sets on classification of high-throughput bacterial 16S rRNA gene surveys. ISME J. **6**:94–103.